Improved Resolution in Proton NMR Spectroscopy of Powdered Solids

Anne Lesage, Luminita Duma, Dimitris Sakellariou, and Lyndon Emsley*

Contribution from the Laboratoire de Stéréochimie et des Interactions Moléculaires, UMR-5532 CNRS/ ENS, Ecole Normale Supérieure de Lyon, 69364 Lyon, France

Received November 15, 2000. Revised Manuscript Received January 30, 2001

Abstract: We present a new solid-state nuclear magnetic resonance experiment that yields, under CRAMPS decoupling conditions, a significant reduction in proton line widths for powdered organic solids. This experiment which relies on a constant-time acquisition of the proton transverse magnetization, removes the contribution of nonrefocusable broadening from the proton line widths. Although this new technique suffers from relatively low sensitivity, we demonstrate in this paper its feasibility on two model samples, L-alanine and the dipeptide Ala-Asp. In both cases a factor of between 2 and 3 in line width reduction is obtained for most of the proton resonances.

1. Introduction

Proton NMR spectroscopy is widely used for the characterization of structure and dynamics of molecules in the liquid state. Due to its high sensitivity, the proton also constitutes an attractive probe nucleus for the study of powdered organic molecules by solid-state NMR. However, in solids the dominant homonuclear proton−proton dipolar interactions lead to broad proton resonances, typically on the order of a few tens of kilohertz for rigid organic solids. This broadening usually obscures any detail in the spectrum such as the chemical shift information (Figure 1a). Thus, one of the current primary challenges in solid-state NMR spectroscopy is to obtain narrow proton line widths. There are currently three distinct approaches to overcome dipolar broadening and obtain high-resolution proton spectra in powdered solids: (i) isotopic dilution with deuterium,[1,2] (ii) fast magic angle spinning (MAS)[3−7] (Figure 1b), and (iii) combined rotation and multiple pulse spectroscopy (CRAMPS)[8−15] (Figure 1c). The first method suffers from the need for complex synthetic procedures, and while it may be a promising possibility for biological systems where isotopic labeling is relatively straightforward, it is not envisagable as a general technique for most organic compounds. Thus, the second and third approaches are currently the most commonly used to

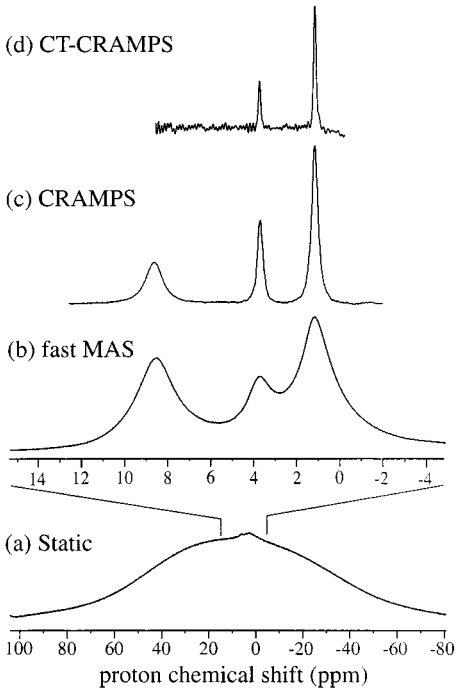

Figure 1. One-dimensional proton spectra of powdered L-alanine. (a) Static spectrum. (b) MAS spectrum at 30 kHz rotor spinning frequency. (c) CRAMPS spectrum under FSLG decoupling at 12.5 kHz rotor spinning frequency. (d) constant-time CRAMPS spectrum under FSLG decoupling at 12.5 kHz rotor spinning frequency. The spectra were acquired at 500 MHz using: (a and b) a one-pulse sequence, (c) the pulse sequence of Figure 2a, (d) the pulse sequence of Figure 2c. See text for details. No weighting functions were applied.

* To whom correspondence should be addressed. E-mail: Lyndon.Emsley@ens-lyon.fr.

(1) McDermott, A. E.; Creuzet, F. J.; Kolbert, A. C.; Griffin, R. G. *J. Magn. Reson*. **1992**, *98*, 408.
(2) Zheng, L.; Fishbein, K.; Griffin, R. G.; Herzlefd, J. *J. Am. Chem. Soc*. **1993**, *115*, 6254.
(3) vanRossum, E. J.; Boender, G. J.; deGroot, H. J. M. *J. Magn. Reson*. **1996**, *120*, 274−277.
(4) Schnell, I.; Brown, S. P.; Low, H. Y.; Ishida, H.; Spiess, H. W. *J. Am. Chem. Soc*. **1998**, *120*, 11784−11795.
(5) Schnell, I.; Lupulescu, A.; Hafner, S.; Demco, D. E.; Spiess, H. W. *J. Magn. Reson*. **1998**, *133*, 61−69.
(6) Saalwdichter, K.; Graf, R.; Spiess, H. W. *J. Magn. Reson*. **1999**, *140*. 471−476.
(7) Yamauchi, K.; Kuroki, S.; Fujii, K.; Ando, I. *Chem. Phys. Lett*. **2000**, *324*, 435−439.
(8) Gerstein, B. C.; Pembleton, R. G.; Wilson, R. C.; Ryan, L. M. *J. Chem. Phys*. **1977**, *66*, 361.
(9) Taylor, R. E.; Pembleton, R. G.; Ryan, L. M.; Gerstein, B. C. *J. Chem. Phys*. **1979**, *71*, 4541−4545.
(10) Burum, D. P.; Rhim, W. K. *J. Chem. Phys*. **1979**, *71*, 944.
(11) Ryan, L. M.; Taylor, R. E.; Paff, A. J.; Gerstein, B. C. *J. Chem. Phys*. **1980**, *72*, 508−515.
(12) Burum, D. P. *Concepts Magn. Reson.* **1990**, *2*, 213−227.
(13) Naito, A.; Root, A.; McDowell, C. *A. J. Chem. Phys*. **1991**, *95*, 3578.
(14) Levitt, M. H.; Kolbert, A. C.; Bielecki, A.; Ruben, D. J. *Solid State NMR* **1993**, *2*, 151−163.
(15) Gerstein, B. C. *The Encyclopedia of NMR*; J. Wiley & Sons: London, 1997; pp 1501−1509.

10.1021/ja0039740 CCC: $20.00
Published on Web 05/25/2001

obtain high-resolution proton spectra. Recently there has been some considerable improvement in the resolution available using these techniques. These improvements have been obtained either for MAS alone, due to technological advances in probe design allowing spinning speeds up to 50 kHz,[16] or for CRAMPS techniques, due to the introduction of improved decoupling schemes.[17−19] Currently, the best proton resolution for organic compounds is obtained using CRAMPS-type techniques in the indirect dimension of a two-dimensional homo- or heteronuclear correlation spectrum,[18,20] and this can yield spectra such as that of Figure 1c. It should be noted that an alternative approach to observing narrow proton line widths has been proposed in the mid 1990s, which consists of single-pulse excitation with delayed acquisition with or without a spin−echo.[21−24] Although interesting, the resulting spectra are believed to correspond to extremely mobile or specially oriented molecules in the solid.[25,26]

In this paper, we show how a factor-two or -three enhancement in resolution can be gained in CRAMPS-type proton spectroscopy of powdered solids by using a two-dimensional constant acquisition time experiment. Using this approach we obtain, for the aliphatic protons of powdered L-alanine, full line widths at half-height as small as 60 Hz (0.12 ppm) (Figure 1d). Similar proton line width reductions are reported for a dipeptide sample.

2. Experimental Section

The powdered samples of L-alanine and the dipeptide Ala-Asp were purchased from Sigma and used without further recrystallization. Approximately 20 mg of each sample was used. The experiments were performed on a Bruker DSX 500 spectrometer (proton frequency 500 MHz) using a conventional triple-resonance 4 mm CP MAS probe. The sample volume was restricted to about 25 μL in the center of the rotor to increase the radio frequency field homogeneity. The rotor spinning frequency was 12.5 kHz for all of the two-dimensional (2D) experiments reported in this paper. Proton−proton homonuclear decoupling was performed using the frequency switched Lee−Goldburg[14,27,28] (FSLG) or the derivative phase-modulated Lee−Goldburg[18] (PMLG) decoupling sequences at a radio-frequency (RF) field strength of 100 kHz. However, other homonuclear decoupling schemes[29] can be employed. In theory, under FSLG or PMLG decoupling, the proton chemical shift is scaled by $1/\sqrt{3}$ (0.57). For both decoupling schemes, the experimental scaling factor was calculated by comparing the ID proton spectra recorded under fast MAS (30 kHz) and under the homonuclear decoupling sequence. Scaling factors of 0.58 and 0.53 were respectively found tor FSLG and PMLG decoupling. The proton chemical shift scale has been corrected for this scaling in all of the spectra reported in this paper, and the proton line widths have been measured on correctly scaled spectra. In the proton dimension, the chemical shift scale was adjusted by recording the proton spectrum of liquid TMS (0 ppm), and under the same spectral conditions, the ID proton spectrum of solid L-alanine and the dipeptide Ala-Asp under fast MAS. The chemical shifts of the CH_3 and OH resonances, which are easily identifiable for L-alanine and the dipeptide Ala-Asp respectively, were measured at 1.18 and 12.58 ppm respectively and then used to reference the 2D spectra. All of the pulse sequences used in this work are available on our web site[30] or by request to the authors.

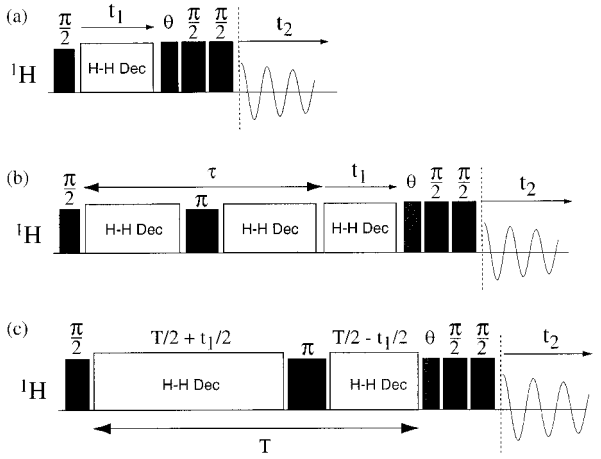

Figure 2. Pulse sequences for the CRAMPS-MAS (a), echo CRAMPS-MAS (b) and constant-time CRAMPS-MAS (c) experiments. Quadrature detection in ω_1 is achieved using the States[45] method by incrementing the phase of the second 90° proton pulse. The first and third 90° proton pulses were cycled independently together with the receiver phase ($+x$, $-x$, and $+x$, $+y$, $-x$, $-y$ for the first and third 90° pulses respectively) yielding an eight-step phase cycle. For the FSLG homonuclear decoupling sequence, θ corresponds to a 54.7° pulse. Detailed pulse programs and phase cycles are available on our website.[30]

3. Mechanisms for Line Broadening

Figure 3 shows the two-dimensional CRAMPS-MAS spectrum of powdered L-alanine acquired using the proton−proton correlation pulse sequence of Figure 2a. This pulse sequence is a modified version of that proposed recently by Vinogradov et al.[18] The first 90° pulse creates the initial proton magnetization in a plane perpendicular to the direction of the effective field present during the application of the multiple-pulse homonuclear decoupling sequence. During t_1, the proton magnetization evolves in this tilted transverse plane under homonuclear decoupling. At the end of the evolution time t_1, a pre-pulse of flip-angle θ is applied which rotates the proton magnetization from the tilted transverse plane to the (x, y) plane of the rotating frame. A z-filter is then applied to allow phase sensitive detection in t_1, before direct signal detection in t_2. This pulse sequence gives a two-dimensional correlation between a high-resolution proton CRAMPS spectrum in ω_1, and the MAS spectrum in ω_2. The one-dimensional CRAMPS spectrum can then be obtained by projection onto the ω_1 axis of the 2D spectrum, or by simply summing the ω_1, traces extracted at the various proton frequencies. This method of indirect detection of the high-resolution proton spectrum is particularly convenient since, first, it allows the use of windowless multiple-pulse sequences which currently have a far superior performance to sequences allowing direct acquisition of the signal. This is especially true for the recently developed windowless homonuclear decoupling sequences such as the PMLG[18] or DUM-

(16) Samoson, A.; Tuherm, T. *The Alpine Conference on Solid-State NMR*; Chamonix-Mont Blanc, 1999.
(17) Hafner, S.; Spiess, H. W. *J. Magn. Reson.* **2001**, *148*, 449−454.
(18) Vinogradov, E.; Madhu, P. H.; Vega, S. *Chem. Phys. Lett.* **1999**, *314*, 443−450.
(19) Emsley, L. In *30th Congress Ampere on Magnetic Resonance and Related Phenomena*; Lisbon, 2000.
(20) Lesage, A.; Emsley, L. *J. Magn. Reson.* **2001**, *148*, 449−454.
(21) Ding, S.; McDowell, C. A. *J. Magn. Reson. A* **1994**, *111*, 212−214.
(22) Ding, S.; McDowell, C. A. *J. Magn. Reson. A* **1995**, *115*, 141−144.
(23) Ding, S.; McDowell, C. A. *J. Magn. Reson. A* **1995**, *117*, 171−178.
(24) Ding, S.; McDowell, C. A. *J. Magn. Reson. A* **1996**, *120*, 261−263.
(25) Fung, B. M.; Tong, T.; Dollase, T.; Magnuson, M. L. *J. Magn. Reson., Ser. A* **1996**, *123*, 56−63.
(26) Gerstein, B. C.; Hu, J. Z.; Zhou, J.; Ye, C.; Solum, M.; Pugmire, R.; Grant, D. M. *Solid State NMR* **1996**, *6*, 63−71.
(27) Bielecki, A.; Kolbert, A. C.; Levitt, M. H. *Chem. Phys. Lett.* **1989**, *155*, 341.
(28) Bielecki, A.; Kolbert, A. C.; deGroot, H. J. M.; Levitt, M. H. *Adv. Magn. Reson.* **1989**, *14*, 111.
(29) Sakellariou, D.; Lesage, A.; Hodgkinson, P.; Emsley, L. *Chem. Phys. Lett.* **2000**, *319*, 253−260.
(30) http://www.ens-lyon.fr/STIM/NMR.

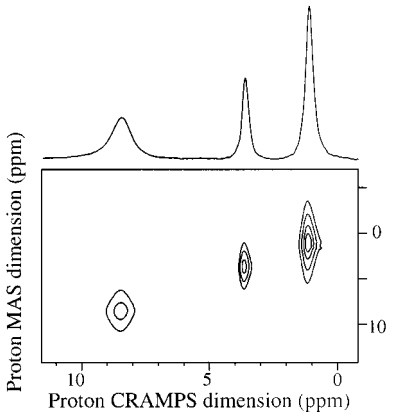

Figure 3. Two-dimensional CRAMPS-MAS spectrum of powdered L-alanine recorded using the pulse sequence of Figure 2a. A total of 512 t_1 points with eight scans each were collected. A spectral width of 26543 Hz was used in the ω_1 dimension. The spinning frequency was 12.5 kHz. The proton RF field strength was set to 100 kHz during t_1 (FSLG decoupling). The ^{1}H CRAMPS spectrum shown above the 2D map was constructed by adding the three ω_1 traces extracted at the CH_3, CH, and NH_3^+ proton frequencies. No signal apodization was applied.

BO1[29] sequences. Moreover this method is much more easily implemented on most modern spectrometers compared to direct detection. In particular quadrature artifacts and axial peaks can be avoided through correct adjustment of the pre-pulse in the sequence, and by phase cycling.

For powdered L-alanine, under our experimental conditions (spinning frequency of 12.5 kHz, and FSLG decoupling at 100 kHz, see the Experimental Section) we measured full line widths at half-height of 170 Hz (0.34 ppm), 150 Hz (0.30 ppm), and 480 Hz (0.96 ppm) for the CH_3, CH, and NH_3^+ proton resonances respectively (we recall that the line widths that we cite in this article are corrected values, the "raw" line widths being smaller by a factor of about 0.57). It is important to realize that these are by no means the limiting or "natural" line widths expected in this system. Indeed, in this kind of crystalline solid, the limiting line width is expected to be less than 10 Hz (although it is in fact difficult to estimate, since it is probably dominated by susceptibility effects). In particular the resolution is still limited by the intrinsic performance of the homonuclear decoupling sequence, that is, the residual proton line broadening under CRAMPS decoupling is mainly due to unaveraged high-order terms of the homonuclear dipolar interaction, or to cross-terms between the homonuclear interaction and the RF field or the chemical shift anisotropy (CSA). To consider alternative methods of eliminating such a broadening, it is important to first characterize the interactions that are responsible for this residual broadening in the effective Hamiltonian obtained under CRAMPS conditions.

These interactions can be divided into symmetric and antisymmetric interactions (such a division is always possible). By symmetric and antisymmetric interactions, we mean interactions that can be described by a Hamiltonian which is invariant (symmetric) or changes sign (antisymmetric) under a π-rotation in spin space.[31] In the following discussion, we will also use the terminology nonrefocusable or refocusable to designate these symmetric and antisymmetric interactions. Thus, a chemical shift distribution corresponds to an antisymmetric interaction, whereas the bilinear terms of, for example, the unaveraged homonuclear

(31) Ernst, R. R.; Bodenhausen, G.; Wokaun, A. *Principles of Nuclear Magnetic Resonance in One and Two Dimensions*; Clarendon Press: Oxford, 1987.

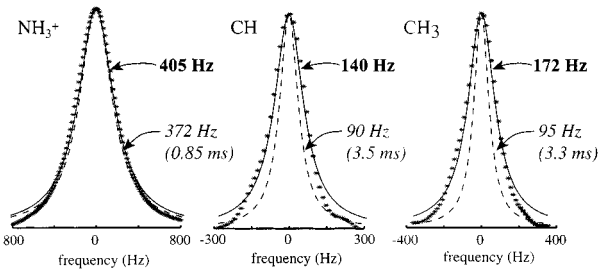

Figure 4. Comparison between the apparent line widths (solid lines) and nonrefocusable line widths (dotted lines) under CRAMPS decoupling conditions for the CH_3, CH, and NH_3^+ protons of powdered L-alanine. The apparent line widths were calculated by fitting, with a Gaussian line shape, the experimental points (indicated by stars) obtained in the ω_1 dimension of the CRAMPS-MAS spectrum of Figure 3. The nonrefocusable line widths are Lorentzian lines calculated from the nonrefocusable dephasing time constant measured using a series of echo CRAMPS experiments (see text for details). The proton RF field strength was set to 100 kHz during the τ period and during t_1 (FSLG decoupling). A total of 17 echo CRAMPS experiments were performed for τ values ranging from 100 μs to 6 ms. The values of the apparent and nonrefocusable full line widths at half-height are indicated for the three types of nuclei, respectively in bold and italic.

dipolar couplings correspond to a symmetric interaction (note that the line broadening due to T_2 relaxation corresponds to a nonrefocusable broadening). The relative contribution of these two types of interaction to the total line width can be investigated by using the pulse sequence of Figure 2b. This is a 2D proton−proton CRAMPS-MAS correlation experiment analogous to the pulse sequence of Figure 2a, but in which the signal acquisition in the CRAMPS dimension starts after a $\tau/2-\pi-\tau/2$ echo period. As the π pulse in the middle of the echo time τ refocuses only the antisymmetric interactions, the amplitude of the peaks in the 2D map as a function of τ will be modulated by the symmetric interactions. Therefore, by recording a series of echo CRAMPS-MAS spectra for different values of the τ period, and by measuring the signal intensity as a function of τ, it is possible to quantify, for each of the resolvable sites in the CRAMPS spectrum, the dephasing time constant due to the symmetric interactions, and hence estimate the contribution of these nonrefocusable interactions to the total line width.

The results obtained for powdered L-alanine are represented schematically in Figure 4. The decay curves for each of the three proton resonances were fitted to a decaying monoexponential function. The corresponding Lorentzian line shape is shown as dashed lines for each of the three sites and compared to the experimentally observed CRAMPS line shape (the experimental points are shown as stars) and to the fit of these points to a Gaussian line shape (shown as a solid line). Note that neither Gaussian nor Lorentzian functions perfectly fitted the data, but they are intended here only as a guide to the order of magnitudes of the different contributions to broadening. As explained above, the dashed line reflects the contribution of the symmetric interactions to the total (or apparent) line width, or in other words, corresponds to the nonrefocusable line width (a term we prefer to the alternative "homogeneous" line width). The full line widths at half-height are indicated in bold for the total line widths and in italic for the nonrefocusable line widths.

The results show that for the NH_3^+ protons of powdered L-alanine the broadening is virtually entirely nonrefocusable. This is likely to be due to effects arising from the coupling with the quadrupolar ^{14}N nucleus. Conversely, for the aliphatic protons (CH and CH_3 groups), roughly 60% of the line width is due to nonrefocusable effects and the remaining 40%, that is, about 60 Hz, corresponds to refocusable interactions. Note

that this distribution is quite different from that obtained in *carbon* spectroscopy under continuous wave decoupling, where we recently showed that the ^{13}C line width is largely dominated by the chemical shift distribution, that is, by refocusable interactions, even for crystalline samples.[32]

For protons, one must note that if the nonrefocusable part is obviously attributable to residual multi-spin interactions, and thus depends on the efficiency of the decoupling, the refocusable part is also likely to be largely dominated by higher-order terms of the residual dipolar interactions, or by cross-terms between the homonuclear interaction and the RF field or CSA which correspond to rank 1 (or 3) spin operators. Thus, even the refocusable line width is expected to depend on experimental parameters such as the spinning speed or the decoupling power. This also means that the limiting line width, which would correspond only to the chemical shift distribution (due to B_0 inhomogeneity, magnetic susceptibility effects, or structural inhomogeneity), is much less than 60 Hz.

In any case, the fact that the line shape is not completely dominated by nonrefocusable terms leads us to envisage in the following section a class of experiments that remove entirely the contribution of these nonrefocusable interactions to the line width.

4. Constant-Time CRAMPS Experiments

Figure 2c shows the pulse sequence for the constant-time CRAMPS-MAS experiment. Constant-time experiments are commonly used in liquid-state NMR spectroscopy to produce ω_1-decoupled spectra.[33−37] In solid-state NMR, constant-time experiments have also been used in carbon spectroscopy to suppress J_{cc} scalar couplings.[38] The only example to date of the use of constant-time experiments to remove dipolar broadening is in an imaging experiment[39] (although the implementation is completely different from that in high-resolution spectroscopy, since B_0 field gradients are used for spatial encoding). In the proton constant-time CRAMPS experiment proposed here, the constant-time principle is used to partly eliminate dipolar broadening from the high-resolution solid-state proton spectrum. Thus, in the sequence of Figure 2c, the acquisition of the signal in t, starts at a constant-time T after the initial 90° proton pulse and a π pulse is shifted from the middle to the end of this constant-time interval progressively from one t_1 increment to another. If the effective Hamiltonian H of the spin system under MAS and decoupling is divided into symmetric $H^{(s)}$ and antisymmetric $H^{(a)}$ parts, the propagator for the pulse sequence can be written as:[40,41]

$$U = \exp\left[-i\frac{T+t_1}{2}(H^{(s)}+H^{(a)})\right]\exp\left[-i\frac{T-t_1}{2}(H^{(s)}-H^{(a)})\right]\exp[-i\pi I_x]$$

Under CRAMPS decoupling conditions, the antisymmetric effective Hamiltonian $H^{(a)}$ can be assimilated to chemical shift like interactions, and in the weak coupling regime, where the shift differences are large compared to the size of the residual symmetric interactions, only the secular components of the symmetric effective Hamiltonian $H^{(s)}$ which commute with $H^{(a)}$ need be retained in the calculation. The propagator can then be simplified to:

$$U = \exp[-iTH^{(s)}]\exp[-it_1H^{(a)}]\exp[-i\pi I_x]$$

Thus, the symmetric interactions, which are insensitive to the position of the π pulse, are active during the whole constant-time T whereas, during t_1, the evolution of the proton magnetization is *only modulated by the antisymmetric interactions*. This implies that the line width obtained in ω_1 will correspond to the refocusable linewidth, whereas the nonrefocusable interactions will only lead to an attenuation of the siginal intensity by a factor which will depend on the terms in $H^{(s)}$ and on the choice of T. In other words, the constant-time CRAMPS experiment should yield a line width reduction by removing the contribution of the nonrefocusable interactions. Note that the simplification in the calculation of the propagator is no longer valid for two coupled proton spins whose chemical shift difference is smaller than the residual nonrefocusable line width. Clearly, the maximum value of t_1 cannot exceed T, and thus constant-time experiments require a compromise between resolution in ω_1 (large values for T to maximize $t_{1,\max}$) and sensitivity (small values of T to minimize loss of signal).

The proton constant-time CRAMPS spectrum of L-alanine (recorded with a T value of 16 ms) is shown in Figure 5a (only the low-frequency part of this spectrum is shown since the NH_3^+ protons give no residual signal). For comparison, the echo CRAMPS spectrum (recorded with the same value of the echo time, 16 ms) and the conventional CRAMPS spectrum are shown in Figure 5b and c, respectively. The full line widths at half-height are indicated on each spectra. PMLG decoupling was used in this series of experiments.

First, we remark that narrower line widths are obtained in the echo CRAMPS spectrum than in the conventional CRAMPS spectrum, that is, a line width reduction can be observed by simply delaying signal acquisition. In fact, since a similar line width reduction is observed in the ω_2 dimension of the 2D maps (for example, for the CH_3 proton, the full line width at half-height in the MAS dimension goes from 1610 Hz in the 2D CRAMPS-MAS spectrum to 1170 Hz in the 2D echo CRAMPS-MAS spectrum, data not shown), we can legitimately assume that the ω_1 line narrowing in the echo CRAMPS experiment is simply related to the fact that this experiment favors the contribution to the signal intensity of the most weakly coupled protons: the signal of the more strongly coupled protons undergoes comparatively greater attenuation through dephasing during the echo time τ than that of the weakly coupled protons. This gain in resolution is of course accompanied by a loss of sensitivity. What is however substantially more interesting is that an additional proton line width reduction is obtained by running the constant-time CRAMPS experiment (Figure 5a). For this experiment, the same ω_2 line widths (1170 Hz for the CH_3 proton resonance in the MAS dimension) as well as the

(32) Lesage, A.; Bardet, M.; Emsley, L. *J. Am. Chem. Soc.* **1999**, *121*, 10987−10993.
(33) Bax, A.; Mehlkopf, A. F.; Smidt, J. *J. Magn. Reson.* **1979**, *35*, 167−169.
(34) Bax, A.; Freeman, R. *J. Magn. Reson.* **1981**, *44*, 542−561.
(35) Rance, M.; Wagner, G.; Sorensen, O. W.; Wutrich, K.; Ernst, R. R. *J. Magn. Reson.* **1984**, *59*, 250−261.
(36) Santoro, J.; King, G. C. *J. Magn. Reson.* **1992**, *97*, 202−207.
(37) Vuister, G. W.; Bax, *A. J. Magn. Reson.* **1992**, *98*, 428−435.
(38) Straus, S. K. In Development and application of techniques for improving resolution in solid-state NMR of fully labelled biomolecules, PhD Thesis ETH Zürich: Zürich, 1998.
(39) Demco, D. E.; Hafner, S.; Kimmich, R. *J. Magn. Reson.* **1992**, *96*, 307−322.
(40) Goldman, M. *Quantum Desciption of High-Resolution NMR in Liquids*; Oxford Science Publications: New York, 1988.
(41) Emsley, L.; Laws, D. D.; Pines, A. In *The Proceedings of the International School of Physics "Enrico Fermi"*, Course CXXXIX; Maragviglia, B. E., Ed.; IOS Press: Amsterdam, 1999.

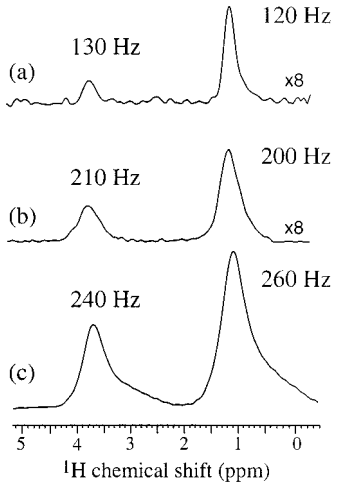

Figure 5. Proton one-dimensional constant-time CRAMPS (a), echo CRAMPS (b) and CRAMPS (c) spectra of powdered L-alanine. These one-dimensional spectra were constructed from two-dimensional spectra. The spinning frequency was 12.5 kHz. The proton RF field strength was set to 100 kHz (PMLG decoupling). The constant-time T and the echo time τ were both set to 16 ms. A total of 16 scans were collected with 256 t_1 points for the normal and echo CRAMPS spectra, and 198 t_1 points for the constant-time CRAMPS spectrum. A spectral width of 10825 Hz was used in the ω_1 dimension.

same signal-to-noise ratio were obtained as for the echo CRAMPS experiment. This indicates that the same "part" of the sample is involved in both experiments and that the observed line width reduction is really due to the constant-time acquisition.

Line widths of 130 and 120 Hz are observed in the constant-time CRAMPS spectrum for respectively the CH and CH_3 protons. This corresponds to a factor of about 2 in line width reduction by comparison to the conventional CRAMPS spectrum of Figure 5c. As mentioned previously, the NH_3^+ protons give no detectable signal. This is because the dephasing time due to the nonrefocusable interactions (0.85 ms) is much shorter than the constant-time T (16 ms) chosen for the experiment. Also we note that, in constant-time experiments, large image peaks appear for each proton resonance at $\omega_H/2$ if the pre-pulses are not correctly adjusted.

As the resolution in the ω_1 dimension of a constant-time CRAMPS experiment is proportional to $1/T$ (since $t_{1,max} = T$), it can be improved by using longer values for the constant-time period T. This is illustrated in Figure 6 which shows constant-time CRAMPS spectra of L-alanine recorded for T values of 16.8, 25.3, and 33.7 ms. For comparison the conventional CRAMPS spectrum is also shown. FSLG decoupling was used in this series of spectra. Note that, under our experimental conditions, the performance of the FSLG decoupling sequence (used in Figure 6) is slightly better than that of the PMLG decoupling sequence (used in Figure 5). In the constant-time experiment recorded with $T = 16.8$ ms the proton line widths are clearly limited by truncation. As expected, the line widths are further reduced by using a longer constant-time period ($T = 25.3$ ms). This gain in resolution is of course at the expense of the signal-to-noise ratio (as mentioned above, a compromise has to be found between resolution and sensitivity in constant-time experiments). No additional line width reduction is observed with a longer constant-time period ($T = 33.7$ ms), which indicates that the resolution limit has been reached in this case.

Finally we present some results of CRAMPS experiments on the dipeptide Ala-Asp, which is a more complex system than

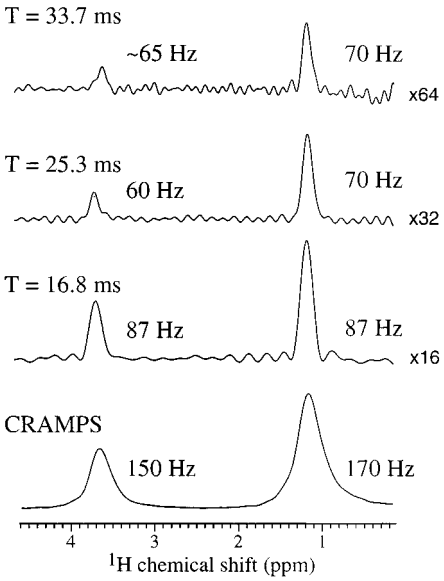

Figure 6. Proton one-dimensional constant-time CRAMPS spectra of powdered L-alanine, recorded with T equal to 16.8, 25.3, and 33.7 ms. The spinning frequency was 12.5 kHz. The proton RF field strength was set to 100 kHz (FSLG decoupling). The conventional CRAMPS spectrum is shown for comparison. These one-dimensional spectra were constructed from two-dimensional spectra recorded with 16 scans per t_1 increment.

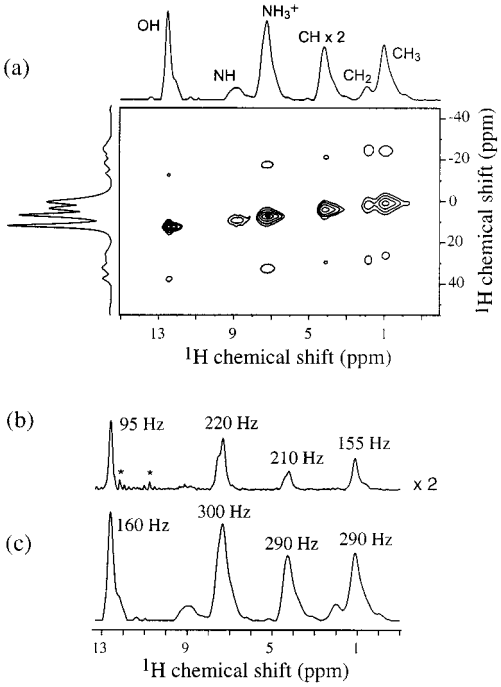

Figure 7. Proton two-dimensional CRAMPS-MAS spectrum (a), and one- dimensional constant-time CRAMPS (b), and CRAMPS (c) spectra for the dipeptide Ala-Asp. The constant-time T was 16.8 ms. The spinning frequency was 12.5 kHz. The proton RF field strength was set to 100 kHz (FSLG decoupling). A total of 32 scans were collected with 512 t_1 points for the normal and echo CRAMPS spectra, and 172 t_1 points for the constant-time CRAMPS spectrum. In the constant-time CRAMPS spectrum, artitfact peaks (appearing at $\omega_H/2$ in ω_1) are indicated by stars.

L-alanine. Figure 7a shows the two-dimensional CRAMPS-MAS spectrum recorded on this sample. The assignment of the proton CRAMPS spectrum, indicated above the 2D map, was obtained from the litterature.[42] The comparison between the conventional CRAMPS spectrum (Figure 7c) and the constant-time CRAMPS

spectrum ($T = 16.8$ ms, Figure 7b) shows that a factor of about 2 can be obtained in line width reduction for the CH_3, CH, NH_3^+, and OH proton resonances. However, the CH_2, and NH resonances are hardly visible in the constant-time spectrum due to the short nonrefocusable dephasing time constants for these resonances. As for the L-alanine sample, better resolution can be obtained with a longer constant-time period (25.2 ms) but at the expense of the spectral intensity (data not shown).

5. Conclusions

In conclusion, in this article we have proposed a new solid-state NMR pulse sequence, the constant-time CRAMPS-MAS experiment, which leads to an additional line narrowing of proton resonances under CRAMPS decoupling conditions. This experiment, which relies on a constant-time acquisition of proton magnetization, yields proton resonances whose line width only derives from refocusable line broadening. The nonrefocusable interactions are removed from the line width and instead modulate the signal intensity. We have applied this technique to a sample of L-alanine, as well as to a dipeptide. In both cases a significant line width reduction was obtained using constant-time CRAMPS experiments by comparison with conventional CRAMPS experiments, which demonstrates the potential of this kind of spectroscopy.

The main shortcoming of the technique is its low sensitivity (as well as the fact that the signal-to-noise ratio can be very different from one peak to another). One must note, however, that the efficiency of constant-time experiments will increase with future improvements in the performance of CRAMPS decoupling sequences. Clearly, the experiment is limited in terms of sensitivity when the nonrefocusable line width is several times larger than the refocusable broadening. Conversely, in disordered materials, where the nonrefocusable broadening is small compared to the refocusable line width, the constant-time CRAMPS experiment will be sensitive but will not yield a change in resolution (although the intrinsic line width will be reduced, which can be possibly exploited in multidimensional correlation experiments). In intermediate cases, proton constant-time spectroscopy represents an attractive technique and is expected to be useful when conventional CRAMPS experiments show insufficient resolution for the unambiguous identification of overlapping resonances. Our demonstrative results indicate that many organic compounds may be in this regime. Consequently, the potential range of applications of this kind of high-resolution proton spectroscopy is very broad. To cite but one example, these experiments should be particularly useful to unravel the structure and dynamics of supramolecular systems where ^1H chemical shifts have recently been shown to be a very sensitive probe.[43,44]

In this paper, the interest of constant-time experiments in proton solid-state NMR spectroscopy is demonstrated particularly to obtain one-dimensional indirect proton CRAMPS spectra, but proton constant-time acquisition periods can also be employed in other experiments, such as multidimensional heteronuclear correlation spectroscopy.

Acknowledgment. We thank Dr. S. Hediger and Dr. P. Hodgkinson for valuable discussions.

JA0039740

(42) Gu, Z.; Ridenour, C. F.; Bronnimann, C. E.; Iwashita, T.; McDermott, A. *J. Am. Chem. Soc.* **1996**, *118*, 822−829.

(43) Brown, S. P.; Schnell, I.; Brand, J. D.; Mullen, K.; Spiess, H. W. *J. Am. Chem. Soc.* **1999**, *121*, 6712−6718.

(44) Brown, S. P.; Schaller, T.; Seelbach, U. P.; Koziol, F.; Ochsenfeld, C.; Klaner, F.-G.; Spiess, H. W. *Angew. Chem.* **2001**. In press.

(45) States, D. J.; Haberkorn, R. A.; Ruben, D. J. *J. Magn. Reson.* **1982**, *48*, 286−292.